Rafał P. JASTRZĘBSKI[1], Olli PYRHÖNEN[2]

Lappeenranta University of Technology (1,2)

Model-based centralized AMB control with position and current feedback and nonlinear observer

***Abstract**. Over the last decade, the model-based position controllers have been investigated in an effort to extend the applicability of the active magnetic bearing (AMB) technology in rotating machinery. This work proposes a very efficient solution to improve the performance of the classical centralized model-based position controller. The article discusses the linear and nonlinear AMB controllers for rigid and flexible rotor models with position and current feedback signals.*

***Streszczenie.** Na przesterzeni ostatniego dziesięciolecia prowadzono badania centralnego sterowania układu zawieszenia magnetycznego w celu zwiększenia zastosowań w aplikacjach maszyn wirujących. Praca ta proponuje skuteczne rozwiązanie, które poprawia sprawność klasycznego centralnego sterownika położenia bazującego na modelu zmiennych stanu. W artykule przedstawione są sterowniki liniowe i nieliniowe dla sztywnego i elastycznego wału oparte na pomiarach położenia i prądu. (**Bazujące na modelu zmiennych stanu centralne sterowanie układu zawieszenia magnetycznego z pomiarami przemieszczeń i prądów w sprzężeniu zwrotnym i z nieliniowym obserwatorem**).*

Keywords: magnetic levitation, active magnetic bearings, optimal control, model-based control, nonlinear control.
Słowa kluczowe: zawieszenie magnetyczne, aktywne łożyska magnetyczne, sterowanie optymalne, sterowanie nieliniowe.

Introduction

The continuous advancement in the capabilities of digital signal processing units provides new opportunities in the application of complex centralized, model-based, and nonlinear controllers to many demanding control systems. The active magnetic bearing (AMB) rotor system is an unstable, nonlinear, multi-input, multi-output, non-collocated plant, which changes its dynamics in time and for different rotational speeds. For the current controlled bearings, the controller layout comprises the inner current loop and the outer position control loop [1]. In the past, the typical industrial controllers included simple decentralized PID-type position controllers [2]. Over the last decade, the more sophisticated model based position controllers have been investigated intensely [1,3,4,5] in an effort to improve the performance and stability and extend the applicability of the AMB technology.

This work proposes a simple, yet very efficient solution to improve the performance of a classical centralized linear quadratic Gaussian (LQG) AMB controller. The LQG control is used as a case study but the presented solutions are extendable to other control synthesis methods, for example to *H*-infinity. The article discusses the controllers for rigid and flexible rotor models. First, the estimated control current signals, which are based on the measured coil currents and rotor displacements, are included to the feedback to model the current limit nonlinearity for the reduced bias current (i_{bias}=2.5☉i_{max}) and to better model the phenomena of attractive force generation. Second, the controller with the nonlinear estimator, which utilizes all the current measurements, is built. The estimators with different number of state variables for representing rotor and actuator states are tested. The proposed solutions are compared with the starting point LQG position feedback controller, which includes basic first-order inner control current loop models The controllers are tested and evaluated using the detailed nonlinear and uncertain plant model.

Plant model

In the studied AMB system there are two eight-pole radial actuators and one axial thrust bearing. The rotor is presented in Fig. 1. The axial suspension is assumed to be decoupled from the radial one. Therefore, we focus on the 4-degrees-of-freedom 4-(DOF) radial suspension. In order to linearize the magnetic force actuator as a function of control current and rotor displacement, a differential driving mode is applied. In this driving mode, each of the eight servodrive reference currents comprises the bias current and the control current such as $i_r = i_0 \pm i_c$.

Before the model-based control is formulated, the practically accurate set of plant models has to be derived. The model used in the controller synthesis cannot be too complex in order to obtain a manageable coupled controller for the implementation [7]. The more detailed nonlinear model is applied to the control validation in simulations in Simulink. For the robust stability analysis, an uncertain plant model is used [5].

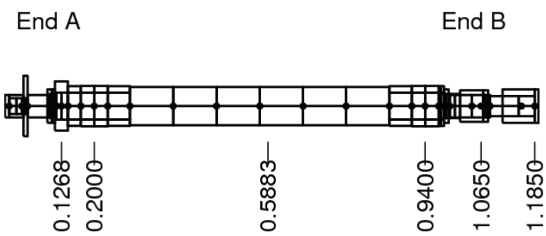

Fig.1. Rotor of the test rig with marked locations (in m, assuming origin in the left end of the rotor): A radial sensor plane, radial AMB, centre point mass, radial AMB, and B radial sensor plane. At the end A there is an axial AMB disc with its corresponding actuator and sensor.

As a starting point for this work for the position control of the classical AMB-rotor system, a plant with four control current inputs $\mathbf{u}=[i_{cxA}, i_{cyA}, i_{cxB}, i_{cyB}]$ and four measured displacement outputs $\mathbf{y}=[x_A, y_A, x_B, y_B]$ is investigated. The investigated alternative plant models extend the outputs by measured eight coil currents.

For the synthesis of the centralized controller, the process is modelled as a linear and time-invariant system. The nominal plant model at standstill consists of the rotor model and the actuator model. The rotor model is obtained using a finite element method (FEM) and corrected based on the results of the experimental modal analysis [5]. Two rotor models are tested. The rigid rotor model comprises the 8 states. In the flexible rotor model, only the lowest frequency mode is retained for the control synthesis. However, the machine is considered to be subcritical. The flexible rotor model comprises 12 states. Two different actuator models are considered. In the first one, the dynamics are modelled using the first-order system approximation for each DOF (4 states). In the second one, each coil current has a separate state variable (8 states).The order of the process model used in the design of the controller is from 12 to 20. We consider the overall plant model [4] in the state variable form as

(1) $$\dot{\mathbf{x}} = \boldsymbol{A}\mathbf{x} + \boldsymbol{B}\mathbf{u} + \boldsymbol{B}_{\mathrm{w}}\mathbf{w}_{\mathrm{n}}, \quad \mathbf{y} = \boldsymbol{C}\mathbf{x},$$

where $\boldsymbol{A}$, $\boldsymbol{B}$, $\boldsymbol{B}_{\mathrm{w}}$, $\boldsymbol{C}$, $\mathbf{x}$, $\mathbf{u}$, $\mathbf{w}_{\mathrm{n}}$, and $\mathbf{y}$ are the state matrix, the input matrix, the disturbance input matrix, the output matrix, the state vector, the input vector, the nonstochastic disturbance input vector, and the output vector, respectively.

The plant model, which is used for the control validation comprises more detailed rotor and actuator models. In the rotor model, the first three bending eigenfrequencies of the rotor are retained. When used for an analytical verification, the total order of the linear part of the process model is 28. Moreover, the non-linear actuator force field model is added. The modelled nonlinearities include: the voltage saturation, the current saturation, the dynamic inductance, and the force-field relation obtained by the reluctance network method (RNM) [6]. Additionally, the pulse width modulation (PWM) delay of the switching actuators is included. The AMB system parameters are shown in Table 1.

Table 1. Key AMB system parameters and their nominal values.

Parameter	Symbol and value
Current stiffness	k_i = 268 NA^{-1}
Position stiffness	k_x = 992 Nmm^{-1}
Rotor mass	m = 46.2 kg
Transverse moment of inertia	I_{xy} = 4.8 kgm^{-2}
Polar moment of inertia	I_z = 0.041 kgm^{-2}
Damping ratio of 1-3 bending modes	0.0041, 0.0022, 0.0043
Frequency of 1-3 bending modes	260 Hz, 539 Hz, 952 Hz
DC link voltage	u_{cd} = 150 V
Bias current	i_{bias} = 2.5 A
Maximum current	$i_{\max}$ = 10 A
Equivalent coil inductance	L = 0.042 H
Equivalent coil resistance	R = 0.43 Ω
Average modulation delay	t_{PWM} = 25 µs
Nominal magnetic air-gap lengths	l_0 = 0.6 mm

Introduction to control design

The starting point for this work is the centralized LQG controller presented in [4] with the unitary weighting matrices when in per-unit (pu) values. In the pus calling the state variables are scaled such that their maximum expected values are 1. The stable suspension in the presence of the rotor bending modes is achieved by applying two different controller configurations. The first one is based on the rigid-body model with the additional sinusoidal disturbance models. The second configuration directly applies the reduced-order FEM rotor model. The both solutions are investigated. For these configurations, the classical linear position feedback controller is compared with the controller with the control current and position feedback and the nonlinear observer (including virtual measurement of the control current). The each control current corresponds to the selected one DOF and is estimated based on two opposite coil currents. Additional version of the estimator with 8 coil currents of the actuator is evaluated. When considering the implementation, the system should be operating in the magnetic centre (effective rotor origin) [8] to best match the simulation results.

LQG control design

In the basic controller layout (Fig. 2), a linear quadratic regulator and state estimator (the steady-state solution of Kalman filter) with an additional constant disturbance observer are built as presented in [4]. The estimator is formed as

(2) $$\begin{bmatrix}\dot{\bar{\mathbf{x}}}\\ \dot{\bar{\mathbf{w}}}_{\mathrm{n}}\end{bmatrix} = \begin{bmatrix}\bar{\boldsymbol{A}} & \bar{\boldsymbol{B}}_w\boldsymbol{C}_{\mathrm{w}}\\ \mathbf{0} & \boldsymbol{A}_{\mathrm{w}}\end{bmatrix}\begin{bmatrix}\bar{\mathbf{x}}\\ \bar{\mathbf{w}}_{\mathrm{n}}\end{bmatrix} + \begin{bmatrix}\bar{\boldsymbol{B}}\\ \mathbf{0}\end{bmatrix}\mathbf{u} + \boldsymbol{L}(\mathbf{y}-\bar{\mathbf{y}}),$$

(3) $$\bar{\mathbf{y}} = \begin{bmatrix}\bar{\boldsymbol{C}} & \mathbf{0}\end{bmatrix}\begin{bmatrix}\bar{\mathbf{x}}\\ \bar{\mathbf{w}}\end{bmatrix}$$

where $\bar{\mathbf{x}}$, $\bar{\mathbf{y}}$, and $\bar{\mathbf{w}}_{\mathrm{n}}$ are the estimate of the state vector, the estimate of the output vector, and the estimate of the disturbance signal, respectively. We assume that the disturbances enter the plant inputs $\boldsymbol{B}_w$=$\boldsymbol{B}$, and that the output matrix of disturbance model $\boldsymbol{C}_{\mathrm{w}}$=$\mathbf{I}$. In the implementation, the state matrix of constant disturbance $\boldsymbol{A}_w$=$\mathbf{0}$. However, for the optimal design of the estimator gain matrix $\boldsymbol{L}$ that provides satisfactory dynamics of the estimation error, the system model (1) is augmented with the perturbed disturbance model. The perturbed disturbance state matrix $\boldsymbol{A}_w$ is diagonal with the elements roughly equal to the selected inverted integrator time constant equal to 0.05s. The estimator gain matrix $\boldsymbol{L}$ is obtained from the steady-state solution of the Riccati equation. The state-feedback is formed by applying the feedback gain matrix $\boldsymbol{K}$ and the disturbance gain matrix $\boldsymbol{K}_{\mathrm{w}}$ as

(4) $$\mathbf{u} = -\boldsymbol{K}\bar{\mathbf{x}} - \boldsymbol{K}_{\mathrm{w}}\bar{\mathbf{w}}$$

The state-feedback controller gain matrix $\boldsymbol{K}$ minimizes the quadratic integral performance index J_{q}, that is

(5) $$J_{\mathrm{q}} = \int_0^\infty \left[\mathbf{x}^{\mathrm{T}}\boldsymbol{Q}\mathbf{x} + \mathbf{u}^{\mathrm{T}}\boldsymbol{R}\mathbf{u}\right]dt,$$

where $\boldsymbol{Q}$, $\boldsymbol{R}$, $\mathbf{x}$, and t are the state weighting matrix, the control weight matrix, the state vector, and time. To determine the diagonal weighting matrices $\boldsymbol{Q}$ and $\boldsymbol{R}$ we utilize the Bryson's rules [9], which result in unitary weighting matrices for both the estimator and control design for the pu system. The disturbance gain matrix $\boldsymbol{K}_{\mathrm{w}}$=$\mathbf{I}$.

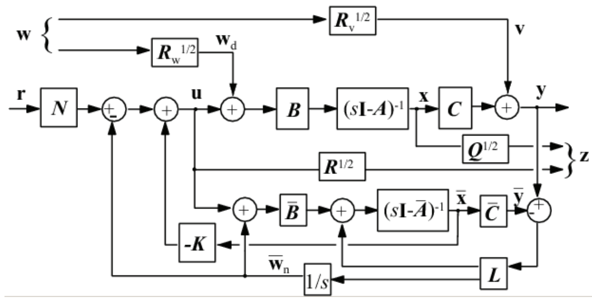

Fig.2. Layout of the LQG controller

It is possible to include more complex disturbance models in the observer. In order to reject the rotor or stator resonances or external periodical disturbance forces, the sinusoidal disturbance model can be included [10]. The inclusion of the sinusoidal disturbance estimate can be viewed as an alternative to the inclusion of the rotor bending eigenmode in the rotor model in the estimator.

Controller with the additional current inputs

The applied control currents, which are considered as the plant outputs $\mathbf{y}$=[i_{cxAm},i_{cyAm},i_{cxBm},i_{cyBm},x_{A},y_{A},x_{B},y_{B}] cannot be measured directly. Instead, they can be estimated as shown in Fig. 3. Assuming the linearized force model, the estimated control current for single DOF is

(6) $$i_{\mathrm{cm}} = \frac{f - k_x x_{\mathrm{b}}}{k_i} = \frac{1}{2}\left(\left|i_{x\mathrm{m}+}\right| - \left|i_{x\mathrm{m}-}\right|\right), \quad f = \frac{k_i}{2}\left(\left|i_{x\mathrm{m}+}\right| - \left|i_{x\mathrm{m}-}\right|\right) + k_x x_{\mathrm{b}},$$

where $i_{x\mathrm{m}+}$ and $i_{x\mathrm{m}-}$ are the measured coil currents in the opposite electromagnets.

The greatest nonlinearities in the plant are present in the actuator. The actuator nonlinearities comprise saturation of current and voltage signals, saturation of iron, dependence of force on currents, positions and temperature. In particular, the current stiffness and position stiffness coefficients can vary significantly from their nominal values when the plant is not in vicinity of the operational point. The LQG observer can be complemented by the nonlinear force model derived in [6], which is applied instead of the constant values of the current stiffness and position stiffness.

The closed-loop control system based on the rigid rotor plant model and without the sinusoidal disturbance model is unstable. However, deriving the sinusoidal disturbance model and control tuning are more difficult in the case of the rigid rotor than the tuning of the controller for the flexible rotor model for the LQG controller.

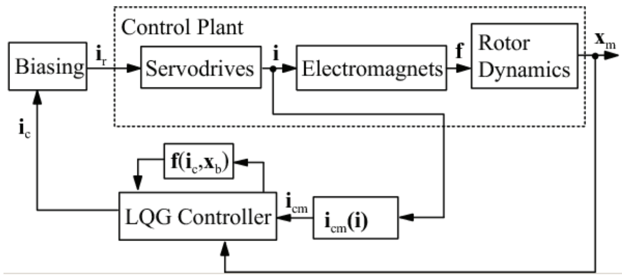

Fig.3. Estimation of vector of the applied control currents $\mathbf{i}_{cm}$ for the flexible rotor model is based on the measured coil currents and the force field model $\mathbf{f}(\mathbf{i}_c,\mathbf{x}_b)$ can be replaced by the nonlinear model for better estimation accuracy

In the most detailed plant model used in the controller synthesis the plant outputs comprise **y** comprise the 8 coil currents 4 displacements. This way, the measured currents are used directly for computing the estimation error and updating the estimated states. In this case, the nonlinear part of the observer consists of eight independent look-up tables, which model the magnetic force dependence on current and position.

Analytical and simulation results

Including the control current measurements as inputs in the centralized position controller improves disturbance rejection and stability compared with the traditional control approach when only positions are measured. The results are verified by simulations of the closed-loop system using the complex and nonlinear plant model. Fig. 4 shows a significantly better step response for the external disturbance force acting on the rotor when comparing position-input feedback controller with position-current-input one.

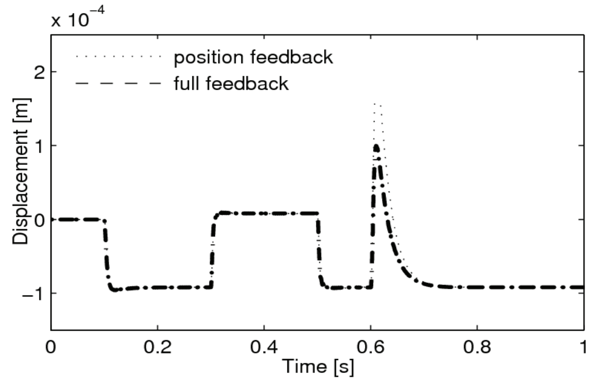

Fig.4. Recorded step reference and disturbance responses (x_A) of the control system with the position feedback and the control system with the position and current feedback

It is interesting to notice that when plotting maximum singular values of the analytical sensitivity functions (Figs 5 and 6) there is no significant difference when the plant is nominal. For the uncertain plant, the closed-loop system is robustly stable when the current feedback is applied in addition to the position feedback (Fig. 7). Fig. 7 presents the singular values of the output sensitivity function. The measured output sensitivity peak is the defined index to measure the system stability [11].

For the controllers based on the rigid rotor model the step responses for the input disturbance (Fig. 8) are further improved in terms of the peak value compared to the controller with the flexible rotor. However, in the response there are oscillations at the frequency corresponding to the first bending mode of the rotor.

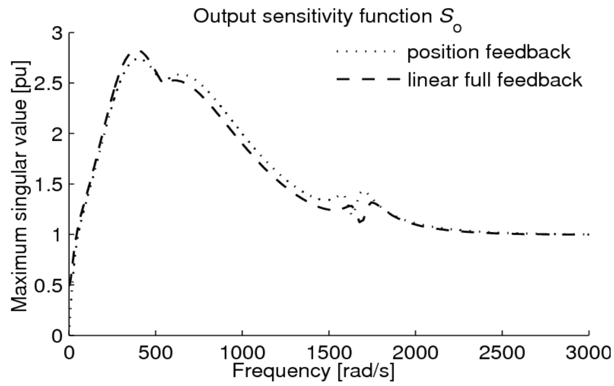

Fig.5. Comparison of the maximum singular values of the output sensitivity functions of the linear controller with the position feedback and the controller with the position and current feedback

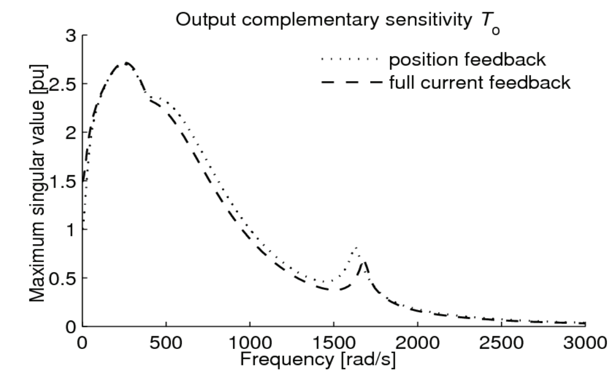

Fig.6. Comparison of the maximum singular values of the output complementary sensitivity functions of the linear controller with the position feedback and the controller with the position and current feedback

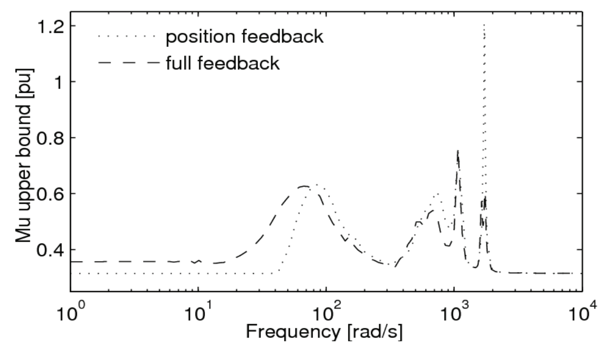

Fig.7. Stability robustness of two closed-loop control designs: the controller with the position feedback signals and the controller with the position and control current feedback

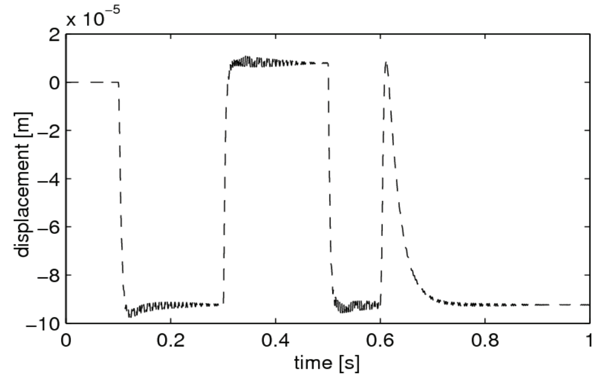

Fig.8. Recorded step reference and disturbance responses (x_A) of the control system with the controller based on the rigid rotor model, sinusoidal disturbance estimator and the position-current feedback

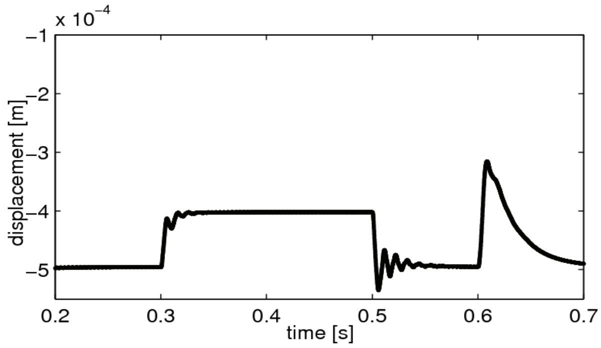

Fig.9. Recorded step reference and disturbance responses (x_A) of the control system with the position feedback and current feedback when far from the operational point

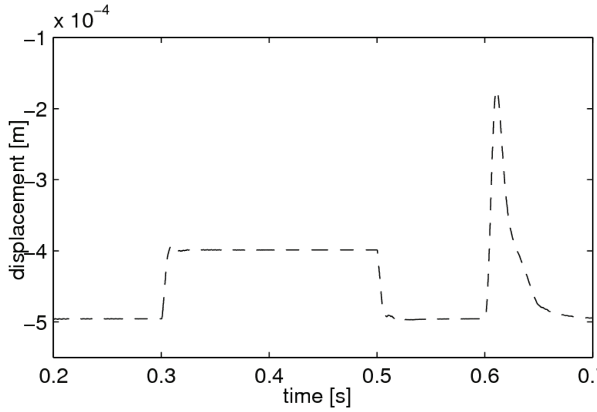

Fig.10. Recorded step reference and disturbance responses (x_A) of the control system with the position current feedback and the nonlinear force model in the observer

Figs. 9 and 10 present the responses when the system is far from the operational point. For the estimator, which includes the linear force model the response is faster but includes oscillations when compared to the response of the controller with the nonlinear force field.

Finally, the controller that includes the most detailed actuator model does not noticeably improve the performance when compared with the controller that incorporates the 4 control currents instead of 8 coil currents.

Conclusions

The performance and robust stability of the AMB closed-loop system can be improved by utilization of all the available measurements in the centralized outer position control loop. The inclusion of control current measurement is simple and efficient. The better performance is not visible for the linear system analysis but is significant when the nonlinear or uncertain plant models are applied. The solution can be extended to other centralized control methods such as H_∞ or μ-synthesis. For the well-identified actuator nonlinearities, the performance can be further increased by applying the nonlinear force observer in the controller. The inclusion of all the measured coil currents as a part of the state variable vector results in marginal improvement when compared to the use of the estimated control currents.

The presented solution requires that the current measurements are available to the outer position controller. The quantitative increase in performance when using all the measured signals in the centralized control instead of the autonomous amplifiers helps the system designer in the selection of suitable hardware configuration.

The future work will include the genetic tuning of the proposed control structure, application to the *H*-infinity design and an experimental evaluation.

REFERENCES

[1] Schweitzer G., Maslen E.H., Editors (2009), Magnetic Bearings: Theory, Design, and Application to Rotating Machinery, Springer, New York.

[2] Polajzer B., Ritonja J., Stumberger G., Dolinar D., Lecointe J-P, Decentralized PI/PD position control for active magnetic bearings. *Electrical Engineering* 89 (2006) No 1, 53–59.

[3] Zhuravlyov Y.N., On LQ-Control of Magnetic Bearing, *IEEE Trans. on Control Systems Technology* 8 (2000) No. 2, 344–350.

[4] Jastrzebski R.P., Pöllänen R., Centralized Optimal Position Control for Active Magnetic Bearings – Comparison with Decentralized Control, *Electrical Engineering* 91 (2009) No. 2, 101–114.

[5] Jastrzebski R.P., Hynynen K., Smirnov A., H-infinity control of active magnetic suspension, *Mechanical Systems and Signal Processing* 24 (2010) No. 4, 995–1006.

[6] Nerg J, Pöllänen R, Pyrhönen J., Modelling the force versus current characteristics linearized parameters and dynamic inductance of radial active magnetic bearings using different numerical calculation methods, *WSEAS Trans Circuit Syst* 4 (2005) No. 6, 551–559.

[7] Bartoszewicz A., Editor (2011) Robust Control / Book 3, InTech, Ch. Discussion on Robust Control applied to Active Magnetic Bearing Rotor System.

[8] Prins R.J., Kasarda M.E.F., Bates Prins S.C., A system identification technique using bias current perturbation for determining the effective rotor origin of active magnetic bearings. *ASME J Vibr Acoust* 129 (2007) 317–22.

[9] Franklin G.F., Powell J.D., Workman M. (1998) Digital control of dynamic systems, 3rd edn. Addison-Wesley, Reading

[10] Jastrzebski, R., Pöllänen, R., (2008) Observer-based unbalance compensation in LQ control of AMBs, In Proc. of ISMB 11, 449–454.

[11] Takahashi, N., Fujiwara, H., Matsushita, O., Ito, M., Fukushima, Y., An Evaluation of Stability Indices Using Sensitivity Functions for Active Magnetic Bearing Supported High-Speed Rotor, *Trans. of the ASME, Journal of Vibration and Acoustics* 129 (2007), 230–238.

***Authors**: Dr Rafał P. Jastrzębski, Prof. Olli Pyrhönen, Dept. of Electrical Engineering, LUT Energy, Lappeenranta University of Technology, PO 20, 53851 Lappeenranta, Finland, e-mails: rafal.jastrzebski@lut.fi, olli.pyrhonen@lut.fi.*